Solid State Dynamics of Tricarbonyl(η-1,5-cyclohexadienylium)iron Tetrafluoroborate and Tricarbonyl(η-1,5-cycloheptadienylium)iron Tetrafluoroborate

Dermot F. Brougham,*,† Patrick J. Barrie,‡ Geoffrey E. Hawkes,§ Isaac Abrahams,§ Majid Motevalli,§ David A. Brown,|| and Gary J. Long⊥

Department of Physics, University of Nottingham, University Boulevard, Nottingham NG7 2RD, United Kingdom, Department of Chemistry, University College London, 20 Gordon Street, London WC1H 0AJ, United Kingdom, Department of Chemistry, Queen Mary and Westfield College, Mile End Road, London E1 4NS, United Kingdom, Department of Chemistry, University College Dublin, Belfield, Dublin 4, Ireland, and Department of Chemistry, University of Missouri—Rolla, Rolla, Missouri 65401-0249

Received December 12, 1995[⊗]

The dynamic behavior of $[(C_6H_7)Fe(CO)_3]BF_4$ (**I**) and $[(C_7H_9)Fe(CO)_3]BF_4$ (**II**) in the solid state has been investigated principally by NMR spectroscopy. High-resolution variable-temperature ^1H and ^{13}C NMR spectra indicate that both complexes have a solid state phase transition above which there is rapid reorientation of the cyclodienylium rings and fast exchange of the carbonyl groups. The transition occurs between 253 and 263 K for **I** and between 329 and 341 K for **II**. The presence of the phase transition is confirmed by differential scanning calorimetry (DSC). ^{57}Fe Mössbauer spectroscopy supports the notion that complex **I** is highly mobile at room temperature, while **II** is relatively static. The activation energy for the cyclodienylium group rotation in the high-temperature phase of **I** is estimated from ^1H spin−lattice relaxation time measurements to be 17.5 kJ mol^{-1}. Static ^{13}C NMR measurements of the solid complexes in the high-temperature phase indicate that the ^{13}C chemical shift anisotropies are only 20−30 ppm. This is significantly less than that expected to result from motion of individual groups and thus suggests that rotation of the whole molecule is involved. A single-crystal X-ray structural determination of complex **II**, at 295 K, showed that the complex is tetragonal (space group $P4_1$, a = 10.610(1) Å, c = 21.761(3) Å, V = 2449.7(5) Å^3, ρ_{calc} = 1.734 g cm^{-3}), with eight cycloheptadienyl cations and eight tetrafluoroborate anions per unit cell. In addition, powder X-ray diffraction studies of both **I** and **II** confirm that at low temperatures both complexes have a tetragonal unit cell, which transforms to a cubic unit cell above the phase transition. The powder patterns, recorded above the phase transition, support the proposal that the complexes are undergoing whole-molecule tumbling in their dynamic regimes.

Introduction

NMR spectroscopy is a powerful tool for the study of dynamic processes in the solid state.[1] Motions in solids may occur with a wide range of correlation times (normally 10^{-1}−10^{-12} s), and such motions can have a profound effect on chemical shifts, anisotropic interactions, and relaxation times. Solid state NMR spectroscopy is therefore uniquely suited for the detection, elucidation, and quantification of these processes.

Often, if a compound contains iron, Mössbauer spectroscopy, which has a characteristic time scale of 10^{-7} s, can be equally useful in the study of solid state dynamic processes. Indeed, several authors have successfully used Mössbauer spectroscopy to study the dynamics of ferrocene and ferrocene-related compounds inserted into a variety of different lattices.[2−8] There have been fewer studies of non-cyclopentadienyl-containing compounds, but Buckingham et al.[9] have reported a preliminary study of a series of cationic tricarbonyl(η-1,5-cyclohexadienyl)-iron complexes, including **I**.

The dynamics of simple organometallic complexes such as transition-metal arene complexes have been extensively studied, and this area has recently been reviewed.[10] Motion in organometallic complexes is important, as it can affect reactivity in the solid state. For example, the solid−vapor reaction of $[P(CH_2CH_2PPh_2)_3Co(N_2)][BPh_4]$ with HCCH, H_2CCH_2, CH_2O, MeCHO, and CO can be rationalized in terms of the motion of the phosphine ligand permitting N_2 elimination and approach of the organic ligand.[11] In the absence of significant internal barriers to motion, the dynamic behavior is determined principally by intermolecular interactions which are a function of molecular shape and crystal packing. The mixed arene−carbonyl complexes (arene)$M(CO)_3$ provide a clear illustration of this. In the case of M = chromium, for instance, it has been

† University of Nottingham.
‡ University College London. Current address: Department of Chemical Engineering, Cambridge University, Pembroke St., Cambridge CB2 3RA, U.K.
§ Queen Mary and Westfield College.
|| University College Dublin.
⊥ University of Missouri—Rolla.
⊗ Abstract published in *Advance ACS Abstracts,* August 1, 1996.

(1) Fyfe, C. A. *Solid State NMR for Chemists*; CFC Press: Ontario, Canada, 1986.
(2) Gibb, T. C. *J. Phys. C* **1976**, *9*, 2627.
(3) Lowery, M. D.; Wittebort, R. J.; Sorai, M.; Hendrickson, D. N. *J. Am. Chem. Soc*. **1990**, *112*, 4214.
(4) Webb, R. J.; Lowery, M. D.; Shiomi, Y.; Sorai, M.; Wittebort, R. J.; Hendickson, D. N. *Inorg. Chem.* **1992**, *31*, 5211.
(5) Fitzsimmons, B. W.; Hume, A. R. *J. Chem. Soc., Dalton Trans.* **1980**, 180.
(6) Maeda, Y.; Ogawa, N.; Takashima, Y. *J. Chem. Soc., Dalton Trans.* **1987**, 627.
(7) Fitzsimmons, B. W.; Sayer, I. *J. Chem. Soc., Dalton Trans.* **1991**, 2907.
(8) Fitzsimmons, B. W.; Marshall, W. G. *J. Chem. Soc., Dalton Trans.* **1992**, 73.
(9) Buckingham, M. J.; Fitzsimmons, B. W.; Sayer, I. *J. Chem. Soc., Chem. Commun.* **1984**, 339.
(10) Braga, D. *Chem. Rev.* **1992**, *92*, 633.
(11) Bianchini, C.; Peruzzini, M.; Zanobini, F. *Organometallics* **1991**, *10*, 3415.

S0020-1669(95)01573-4 CCC: $12.00

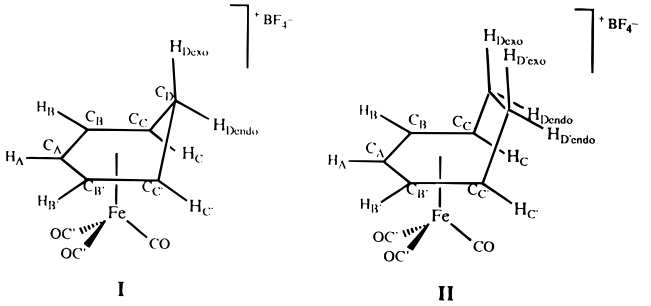

Figure 1. The complexes $[(C_6H_7)Fe(CO)_3]BF_4$ (**I**) and $[(C_7H_9)Fe(CO)_3]BF_4$ (**II**).

found that, in $(C_6H_6)Cr(CO)_3$, the benzene ring undergoes rapid reorientation about a 6-fold rotation axis at room temperature, while, in $(C_6H_5Me)Cr(CO)_3$, the aromatic unit is believed to be static, on the NMR time scale, at least.[12] This occurs because the arene rings do not physically obstruct each other in the benzene complex, whereas the methyl group of the less symmetric toluene complex protrudes and hinders the motion of the ring in the solid state.[10] Similarly, NMR studies have shown that the activation barrier to a $2\pi/5$ rotation in ferrocene is 13.5 kJ mol^{-1} whereas the barrier for monosubstituted ferrocene derivatives (η^5-C_5H_4R)Fe(η^5-C_5H_5) is substantially higher; for example if R = COMe (acetylferrocene), the barrier is 46.0 kJ mol^{-1}.[13] Complexes involving larger rings have also being studied, most notably complexes of cyclooctatetraene.[14]

With the exception of one preliminary report,[9] there have as yet been no studies of complexes involving expanded η^5-cyclodienylium rings such as the cyclohexadienyl, η^5-C_6H_7, and cycloheptadienyl, η^5-C_7H_9, ligands. In this work, we present a study of the dynamics of the complexes $[(\eta^5\text{-}C_6H_7)Fe(CO)_3]BF_4$ (**I**) and $[(\eta^5\text{-}C_7H_9)Fe(CO)_3]BF_4$ (**II**) in the solid state; see Figure 1. The chemistry of these complexes has proven of interest due largely to the stereoselectivity and regioselectivity of their reactions with nucleophiles.[15,16] In addition, numerous attempts, both experimental and theoretical, have been made to understand their geometric deformations,[17,18] their reactivity,[19] their solution NMR spectra,[20] and the fluxionality of their rings in solution.[21] In the solid state it might be expected that the asymmetric rings would hinder any reorientational process and that this might be a function of the number of methylene groups present. In fact, the solid state NMR spectra reported in this work show, surprisingly, that there is rapid motion in these complexes, even at moderate temperatures.

Experimental Section

The NMR spectra were obtained at 75.47 MHz for ^{13}C and 300.13 MHz for ^{1}H on a Bruker MSL-300 using magic-angle spinning (MAS) and high-power proton decoupling. Cross-polarization (CP) was used to obtain the ^{13}C spectra. The 90° pulse length was typically 4.3 × 10^{-6} s for ^{1}H and ^{13}C. Spinning rates were typically 4.5 kHz. The temperature was controlled using a Bruker VT-1000 unit; the thermocouple was calibrated on the basis of the temperature-dependent chemical shifts of samarium acetate (for low temperatures) and on the basis of phase transitions (for high temperatures).[22] Despite this calibration, the error in the temperature may be as much as 5 K at some temperatures due to the uncertainties associated with frictional heating of the rotor and the effect of the rf decoupling field. Differential scanning calorimetry data was obtained using a Shimadzu DSC-50. Mössbauer spectra were obtained with a conventional constant-acceleration spectrometer, which utilized a room-temperature rhodium matrix cobalt-57 source and was calibrated by using room-temperature α-iron foil. With the exception of the 295 K spectrum of **I**, the spectra were fitted with asymmetric quadrupole doublets with a Lorentzian line shape by using standard least-squares computer minimization techniques. The 295 K spectrum of **I** was fitted with a single broadened symmetric Lorentzian line.

Table 1. Crystallographic Data for $[(C_7H_9)\ Fe(CO)_3]BF_4$ (**II**)

empirical formula $C_{10}H_9BF_4FeO_3$	fw 319.83
$a = 10.6100(10)$ Å	space group $P4_1$ (No. 76)
$b = 10.6100(10)$ Å	$T = 293(2)$ K
$c = 21.761(3)$ Å	$\lambda = 0.710\ 69$ Å
$V = 2449.7(5)$ Å^3	$\rho_{calcd} = 1.734$ g/cm^3
$Z = 8$	$\mu = 1.280$ nm^{-1}
$R(F_o^2)$ [$F > 4\sigma(F)$] = 0.0642[a]	$R(F_o^2)$ (all data) = 0.0908
$R_w(F_o^2)$ [$F > 4\sigma(F)$] = 0.1813[b]	$R_w(F_o^2)$ (all data) = 0.1934

[a] $R_1 = \sum||F_o| - |F_c||/\sum|F_c|$. [b] $R_w = [\sum[w(F_o^2 - F_c^2)^2]/\sum[w(F_o^2)^2]]^{1/2}$. Calculated weight $w = 1/\sigma^2(F_o^2) + (0.1481P)^2 + 0.0000P]$ where $P = (F_o^2 + 2F_c^2)/3$.

Attempts to grow crystals of **I** were unsuccessful. Single crystals of **II** were grown from a solution of CH_3CN/Et_2O (90:10) at room temperature. The solid state structure, at room temperature, of **II** was solved. Data were collected on an Enraf-Nonius CAD-4 diffractometer at room temperature. Data collection parameters are given in Table 1. The structure was solved by Patterson methods using SHELXS-86[23] and refined using SHELXL-93.[24] Anisotropic thermal parameters were refined for all non-hydrogen atoms by full-matrix least-squares calculations on F^2. Hydrogen atoms were refined in geometrically idealized positions using an atom riding model. An empirical absorption correction was applied to the data prior to refinement.

X-ray powder diffraction data were collected for **I** and **II** on a Siemens D5000 diffractometer in flat-plate geometry, using graphite-monochromated Cu Kα ($\lambda = 1.5418$ Å) radiation. Data were collected at room temperature for both **I** and **II** and also at 353 K for sample **II**.

Results

^{1}H NMR Spectra. The ^{1}H MAS NMR spectrum of the η^5-C_6H_7 complex, **I**, at room temperature is shown in Figure 2. Five peaks are resolved, at 7.2, 5.8, 4.2, 3.0, and 2.0 ppm, and the chemical shifts agree well with those observed in solution;[25] these resonances correspond to H_A, H_B and $H_{B'}$, H_C and $H_{C'}$, H_{D-exo}, and H_{D-endo}, respectively (with the labels shown in Figure 1). Spectral deconvolution confirms that the intensities are in the expected ratio of 1:2:2:1:1. The most notable feature of the spectrum is the exceptionally high resolution achieved at a spinning rate of 4.5 kHz. Given that the dipolar interactions are expected to be of the order of 60 kHz,[1] this implies that there must be rapid reorientation of the cyclodienylium ring in **I** at room temperature. On lowering of the temperature to 263 K, the resolution of the peaks is lost due to broadening of the signals and the intensities of the spinning sidebands increase. By 243 K, the ^{1}H MAS NMR spectrum consists of a single

(12) Lucazeau, C.; Chhor, K.; Sourisseau, C.; Dianoux, A. *J. Chem. Phys.* **1983**, *76*, 307.
(13) Freyberg, D. P.; Robbins, J. L.; Raymond, K. N.; Swart, J. C. *J. Am. Chem. Soc.* **1979**, *101*, 892.
(14) Campbell, A. J.; Cottrell, C. E.; Fyfe, C. A.; Jeffrey, K. R. *Inorg. Chem.* **1976**, *15*, 1321.
(15) Jones, D.; Pratt, L.; Wilkinson, G. *J. Chem. Soc.* **1962**, 4458.
(16) Fischer, E. O.; Fischer, R. D. *Angew. Chem.* **1960**, *72*, 919.
(17) Hoffmann, R.; Hofmann, P. *J. Am. Chem. Soc.* **1976**, *98*, 598.
(18) Brown, D. A.; Fitzpatrick, N. J.; McGinn, M. A. *J. Chem. Soc., Dalton Trans.* **1986**, 701.
(19) Clack, D. W.; Monshi, M.; Kane-McGuire, C. A. P. *J. Organometallics Chem.* **1976**, *107*, C40.
(20) Dobosh, P. A.; Gresham, D. G.; Kowalski, D. J.; Lillya, C. P.; Magyar, E. S. *Inorg. Chem.* **1978**, *17*, 1775.
(21) Whitesides, T. H.; Lichtenberger, D. L.; Budnik, R. A. *Inorg. Chem.* **1975**, *14*, 68.
(22) Haw, J. F.; Campbell, G. C.; Crosby, R. C. *Anal. Chem.* **1986**, *58*, 3172.
(23) Sheldrick, G. M. *Acta Crystallogr.* **1990**, *A46*, 467.
(24) Sheldrick, G. M. *Program for the Refinement of Crystal Structures*; University of Göttingen: Göttingen, Germany, 1993.
(25) Brookhart, M.; Harris, D. L. *Inorg. Chem.* **1974**, *13*, 1540.

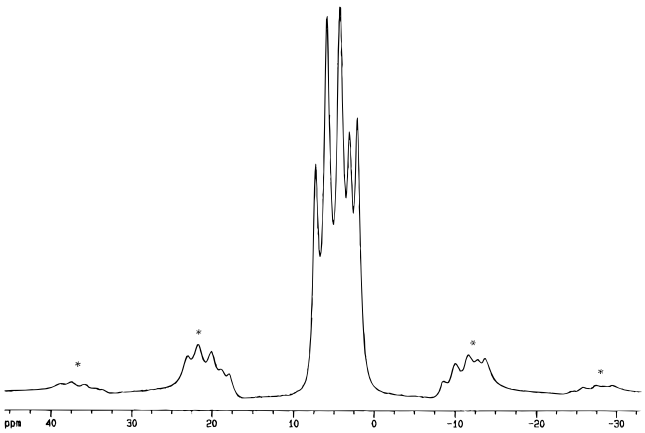

Figure 2. ^{1}H MAS NMR spectrum of **I**, at 295 K (spin rate 4.7 kHz). Spinning sidebands are marked by asterisks.

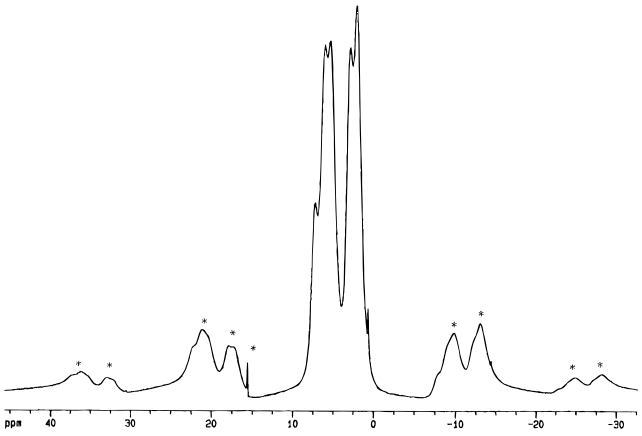

Figure 3. ^{1}H MAS NMR spectrum of **II**, at 390 K (spin rate 4.7 kHz). Spinning sidebands are marked by asterisks.

broad peak with a half-width of ca. 60 kHz, indicating that the motion has ceased.

In contrast, the line width in the ^{1}H MAS NMR spectrum of the η^5-C_7H_9 complex, **II**, at room temperature shows that the ring is static. However, when the temperature is raised to 329 K, a high-resolution ^{1}H spectrum is obtained, indicating that the complex is highly mobile at this temperature. The spectrum at 390 K is shown in Figure 3 and consists of five resonances at 7.1, 5.9, 5.2, 2.7, and 2.0 ppm in the intensity ratio 1:2:2:2:2. The chemical shifts are once again close to the values observed in solution NMR spectra[25] and thus the resonances are assigned to H_A, H_B and $H_{B'}$, H_C and $H_{C'}$, H_{D-exo} and $H_{D'-exo}$, and H_{D-endo} and $H_{D'-endo}$, respectively.

^{13}C NMR Spectra. The ^{13}C CP/MAS NMR spectrum of **I** at 243 K shows the behavior expected of a static system. There are two carbonyl resonances in a 2:1 ratio at 201.5 and 210.6 ppm, respectively. Simulation of the intensities of the spinning sidebands indicates that the ^{13}C shielding tensor is axially symmetric with an anisotropy of 390 ppm, which is in the expected range for static terminal carbonyl groups.[26] The cyclodienylium resonances are at 102.5, 90.9, 62.7, and 23.9 ppm and are assigned to C_A, C_B and $C_{B'}$, C_C and $C_{C'}$, and C_D, respectively, again in agreement with solution NMR data.[27] The detection of two carbonyl peaks and four cyclodienylium peaks would be consistent with a mirror plane passing through one of the Fe−C−O units. Between 253 and 263 K (see Figure 4), there is a general sharpening of the resonances with the carbonyl

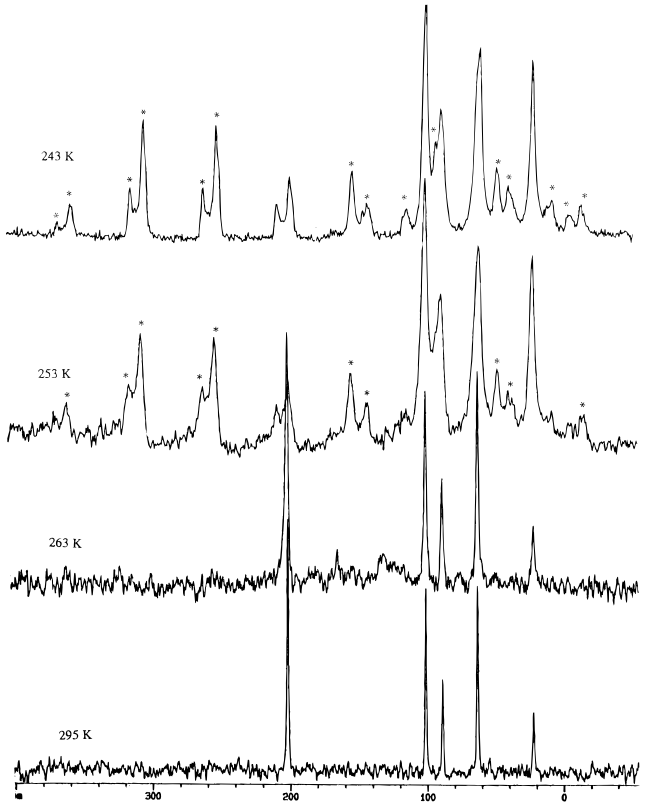

Figure 4. ^{13}C CP/MAS NMR spectra of **I**, at 243 (top), 253, 263, and 295 K (spin rate 4.0−4.5 kHz). Spinning sidebands are marked by asterisks.

signal becoming a single sharp peak at 202.9 ppm. This chemical shift is somewhat different from that observed in solution (212.9 ppm), which may reflect motion between different sites (staggered/eclipsed with respect to the cyclodienylium ring) in the solid and in solution. Above 263 K, the spinning sidebands of the carbonyl resonance disappear completely as do those of the cyclodienylium ring, whose peaks are now completely resolved. It is thus clear that there is fast dynamic averaging of the chemical shift anistropy (CSA).

At room temperature the ^{13}C CP/MAS spectrum of **II** is as expected for the static system: the carbonyl resonances are at 200.8 and 208.2 ppm (2:1 intensity ratio); the cyclodienylium resonances are at 103.4, 101.6, and 93.8 ppm for C_A, C_B and $C_{B'}$, and C_C and $C_{C'}$ and at 34.5 and 29.1 ppm for the methylene carbons C_D and $C_{D'}$. As there are two chemical environments for the methylenes at this temperature, there cannot be a mirror plane through the molecule, although the fact that two of the carbonyl groups give coincident chemical shifts may indicate an approximate mirror plane. Again the chemical shifts are similar to those reported in solution, except that in solution the carbonyls and the methylenes are chemically equivalent.[27] When the temperature is raised, dynamic behavior, similar to that described above for **I**, begins (see Figure 5). At 319 K, the isotropic carbonyl resonance has increased in intensity relative to the spinning sidebands and a third methylene resonance appears at 32.0 ppm (between the two original methylene peaks). Such behavior is typically the result of a phase transition rather than peak coalescence. The relative intensity of the peaks continues to change as the temperature is increased until at 329 K the new phase dominates. By 341 K, the spectrum of **II** indicates a pure phase with no detectable spinning sidebands. Note that the carbonyls and the rings become motional over the same temperature range, and thus

(26) Hawkes, G. E.; Sales, K. D.; Aime, S.; Gobetto, R.; Lian, L. Y. *Inorg. Chem.* **1991**, *30*, 1489.
(27) Olah, G. A.; Yu, S. H.; Liang, G. *J. Org. Chem.* **1976**, *41*, 2383.

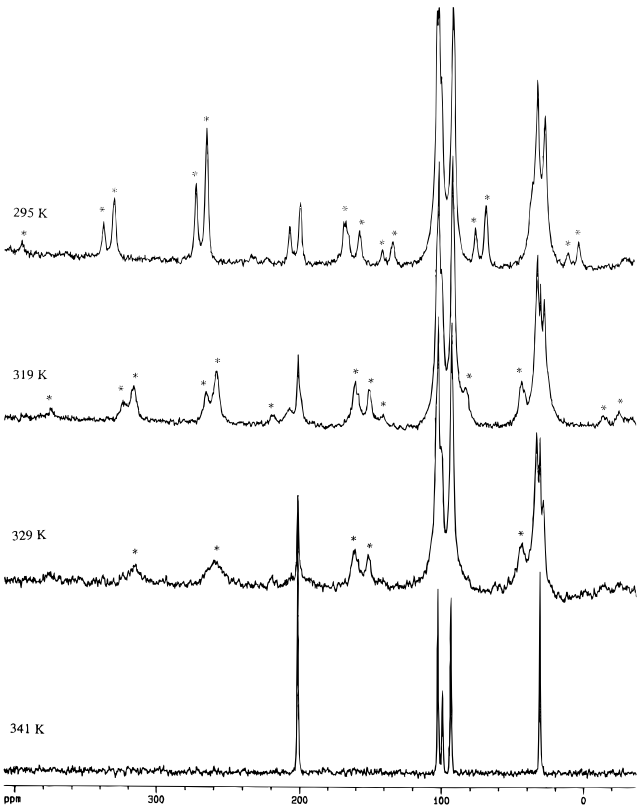

Figure 5. ^{13}C CP/MAS NMR spectra of **II**, at 295 (top), 319, 329, and 341 K (spin rate 4.0−4.5 kHz). Spinning sidebands are marked by asterisks.

not only are they both dynamic in the high temperature regime, but their motions may be correlated in some way.

The absence of spinning sidebands for the ^{13}C carbonyl resonances of the high-temperature phases of **I** and **II** is of note as it indicates that the averaged chemical shift anisotropy is close to zero. This does not necessarily imply whole-molecule tumbling. Fast 3-fold exchange of the carbonyl sites is equivalent to rotation about the axis between the iron atom and the center of the η^5 ring. In the event that the angle of this rotation is close to the magic angle, a substantial reduction of the shielding anisotropy will be observed provided that the rate of exchange is much greater than the magnitude of the shielding anisotropy. For instance, fast three-site exchange between identical CO sites with axially symmetric shielding tensors is expected to result in a shielding tensor with anisotropy, $\Delta\sigma'$, which is modified from the static anisotropy, $\Delta\sigma$, by the factor $(3\cos^2\theta - 1)/2$ (where θ denotes the angle between the CO bond and the axis of rotation). In principle, this relationship can be used to obtain structural information.[28] In the case of complexes **I** and **II** in their high-temperature phases, slow spinning or static ^{13}C NMR spectra show that the ^{13}CO shielding anisotropy is less than 25 ppm, and it is not possible to obtain the sign of the anisotropy with any confidence. This might suggest that the angle θ about which CO rotation occurs is close to the magic angle (at which $\theta = 54.7°$ and $(3\cos^2\theta - 1)/2 = 0$). However, the slow-spinning and static ^{13}C NMR spectra also show that the anisotropies of the cyclodienylium carbons have been greatly reduced, again to less than 25 ppm. The chemical shift anisotropies of static cyclodienylium carbons are normally >100 ppm, and the ^{13}C spectra of **I** and **II** at low temperatures are consistent with this. Rapid motion around the axis between the iron atom and the center of the η^5 ring would only be expected to reduce the magnitude of the ^{13}C shielding tensor by a factor of about 2. Hence the low anisotropies observed indicate some more complex whole-molecule motion must be occurring.

^{1}H Spin−Lattice Relaxation Time Measurements. Spin−lattice relaxation times are sensitive to molecular motions with frequencies in the range 10^7-10^{10} s^{-1}, and in favorable cases it is possible to obtain quantitative information about the activation barrier to the motion.[1,29,30] Variable-temperature ^{1}H T_1 experiments were performed on the high-temperature phases of both **I** and **II**. However, considerable difficulty was experienced in obtaining reliable data, as the ^{1}H T_1 values obtained depended on the samples' thermal history. While the sample decomposition temperature is above 470 K for both samples, heating above 370 K caused small but significant irreversible changes in ^{1}H spin−lattice relaxation time, possibly due to trace amounts of paramagnetic species being formed. Any partial decomposition occurring between 370 and 400 K must, however, be small, as the ^{1}H and ^{13}C NMR spectra were unaffected apart from a slight increase in spinning sideband intensities. Fitting the measured ^{1}H T_1 values for **I** between 263 and 370 K to the standard expression of Kubito and Tomita[29] gave a correlation time for the motion of 4.3×10^{-9} s at 298 K and an activation barrier of 17.5 kJ mol^{-1}. Given the fact that irreproducible behavior was observed above 370 K and that the frequency dependence of the ^{1}H relaxation times was not explored, these values should be viewed as estimates rather than accurate measurements. The small temperature range available above the phase transition for **II** but before irreversible changes in T_1 occurred prevented quantitative analysis of relaxation times for this sample.

Mössbauer Spectra. The Mössbauer spectra of complexes **I** and **II** at 78 and 295 K are shown in Figure 6, and the hyperfine parameters corresponding to the fit shown are given in Table 2. The spectra confirm that there is a difference in the ^{57}Fe environments of **I** and **II** at room temperature. The Mössbauer spectral parameters for **I** at 78 K and for **II** at 78 and 295 K are typical of non-cyclopentadienyl-containing organometallic complexes of this type[9,31−34] and indicate normal static behavior at these temperatures. In contrast, at 295 K, **I** exhibits a weak broadened line typical of dynamic behavior[2] and has hyperfine parameters virtually identical to those reported earlier.[9] The broadened line results from the rapid interchange of ligands relative to the 1×10^{-7} s lifetime of the ^{57}Fe excited state.[35] Thus the Mössbauer spectra confirm that, at room temperature, complex **I** is motional and complex **II** is static. This conclusion is further supported by the temperature dependence of the isomer shift, δ, and the Mössbauer spectral absorption area.[36,37] The observed effective recoil-free masses, M_{eff}, reported in Table 2 are typical of the high covalency expected of the iron−ligand bonds found in these com-

(28) Barrie, P. J.; Mitsopoulou, C. A.; Randall, E. W. *J. Chem. Soc., Dalton Trans.* **1995**, 2125.
(29) Kubito, R.; Tomita, K. *J. Phys. Soc. Jpn.* **1954**, *9*, 888.
(30) Andrew, E. R. *Nuclear Magnetic Resonance*; Cambridge University Press: Cambridge, U.K., 1958; p 167.
(31) Benson, C. G.; Long, G. J.; Bradley, J. S.; Kolis, J. W.; Shriver, D. F. *J. Am. Chem. Soc.* **1986**, *108*, 1898.
(32) Grandjean, F.; Long, G. J.; Benson, C. G.; Russo, U. *Inorg. Chem.* **1988**, *27*, 1524.
(33) Buhl, M. L.; Long, G. J.; O'Brien, J. F. *Organometallics* **1993**, *12*, 1902.
(34) Cassidy, J. C.; Whitmire, K. H.; Long, G. J. *J. Organomet. Chem.* **1992**, *427*, 355.
(35) Atkins, P. W. *Physical Chemistry*, 3rd ed.; Oxford University Press: Oxford, U.K., 1986; p 500.
(36) Herber, R. H. *Chemical Mössbauer Spectroscopy*; Herber, R. H., Ed.; Plenum: New York, 1984; pp 199−216.
(37) Ernst, R. D.; Wilson, D. R.; Herber, R. H. *J. Am. Chem. Soc.* **1984**, *106*, 1646.

Table 2. Mössbauer Spectral Parameters

compound	T, K	δ,[a] mm s^{-1}	ΔE_Q, mm s^{-1}	Γ, mm s^{-1}	area (%E), mm s^{-1}	M_{eff}, g mol^{-1}	θ_m, K
$[(\eta^5\text{-}C_6H_7)Fe(CO)_3]BF_4$ (**I**)	295	0.030	0	1.00	0.34	109	70
	78	0.113	1.55	0.25	8.07		
$[(\eta^5\text{-}C_7H_9)Fe(CO)_3]BF_4$ (**II**)	295	0.026	1.51	0.25	2.54	117	98
	78	0.103	1.54	0.25	11.03		

[a] Relative to room temperature α-iron foil.

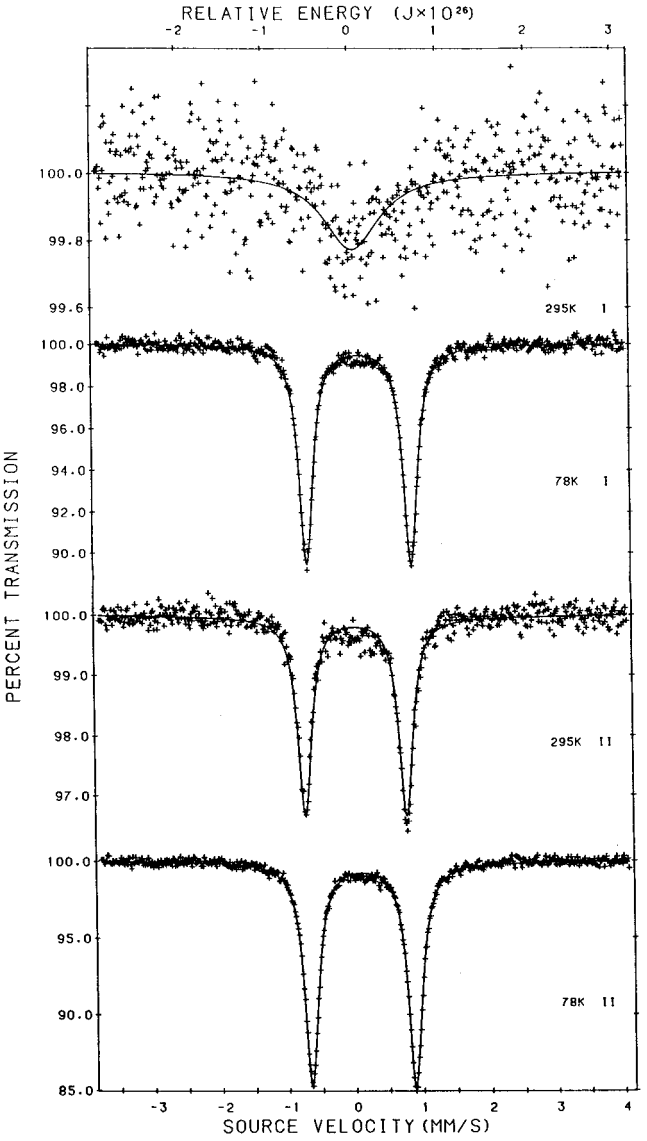

Figure 6. Mössbauer spectra of **I** and **II** at 78 and 295 K.

pounds.[34,37] In contrast, the Mössbauer lattice temperatures, θ_M, determined from the spectral results at 295 and 78 K as explained by Ernst et al.,[37] are quite low, especially in the case of **I**. These θ_M values are found in the range 130−160 K for a series of bis(pentadienyl)iron compounds[37] and are typically above 100 K.[34] Thus the small value found for **I** indicates that it has the nonrigid type of lattice required for motional behavior at room temperature. Even though these results should be considered preliminary because they are based on only two temperatures,[38] they are completely consistent with the dynamic properties observed for these compounds. A detailed study of the temperature dependence of the Mössbauer spectra of **I**, **II**, and related compounds will be undertaken in the near future.

(38) Buhl, M. L.; Long, G. J.; O'Brien, J. F. *Organometallics* **1993**, *12*, 283.

Table 3. Fenske−Hall Molecular Orbital Calculations for Complex **II**

	iron site	
	Fe(1)	Fe(2)
HOMO/LUMO gap, eV	9.22	10.20
3d orbital population	6.89	6.92
4s orbital population	0.17	0.17
4p orbital population	0.06	0.06
charge	+0.35	+0.34
Slater effective nuclear charge	3.14	3.12
Clementi effective nuclear charge	4.64	4.62
quadrupole splitting, mm s^{-1}	−1.55	−1.46

It is interesting that the Mössbauer spectrum of **II** gives such narrow line widths in view of the presence of the two crystallographically distinct iron sites observed in its crystal structure; see below. This indicates that both electronically and structurally the two sites are very similar. This similarity has been confirmed by a Fenske−Hall molecular orbital study of the two different iron-containing cations. The results are presented in Table 3 and reveal very similar, but not identical, Mulliken populations for the two iron sites. In earlier work[38−40] on a series of organoiron clusters containing metal−metal bonds, it was shown that there is a good correlation between the sum of the Mulliken iron 4s orbital population and the Clementi effective nuclear charge and the observed isomer shift. The calculated values given in Table 3, in conjunction with this correlation, predict a somewhat higher ^{57}Fe Mössbauer isomer shift than is observed. However the calculated and observed isomer shifts are in good agreement with the results obtained for a series of oranoiron compounds that do not contain metal−metal bonds.[41] The calculated quadrupole splittings are negative for both sites and are in excellent agreement with the observed splitting whose sign cannot be determined from the observed spectrum. The very narrow line widths observed in the Mössbauer spectrum of **II** reveal that the spectrum is not sensitive to the small electronic differences revealed in Table 3.

Differential Scanning Calorimetry. The presence of phase transitions implied by the NMR data discussed above was confirmed by differential scanning calorimetry (DSC); see Figure 7. When fresh samples of **I** and **II** were heated from low temperature, single endotherms due to phase transitions were detected, prior to melting/decomposition (*ca*. 473 K). For **I** the endotherm was centered at 259 K, with an enthalpy change of 6.14 kJ mol^{-1}. For **II** the endotherm was centered at 339 K, with an enthalpy change of 11.00 kJ mol^{-1}. At the heating rate used (10 K/min) the endotherm for **I** was 20 K wide (250−270 K), while for **II** it was 15 K wide (331−346 K). The transition temperatures measured by DSC agree well with the NMR data, which indicated structural transitions at 253−263 and 329−341 K for **I** and **II**, respectively.

DSC measurements were also made on samples of **I** and **II** which had been heated to 423 K for 30 min in order to explore

(39) Buhl, M. L.; Long, G. J. *J. Organomet. Chem.* **1993**, *461*, 177.
(40) Buhl, M. L.; Long, G. J.; Doyle, G. *J. Organomet. Chem.* **1993**, *461*, 187.
(41) Long, G. J. Unpublished results.

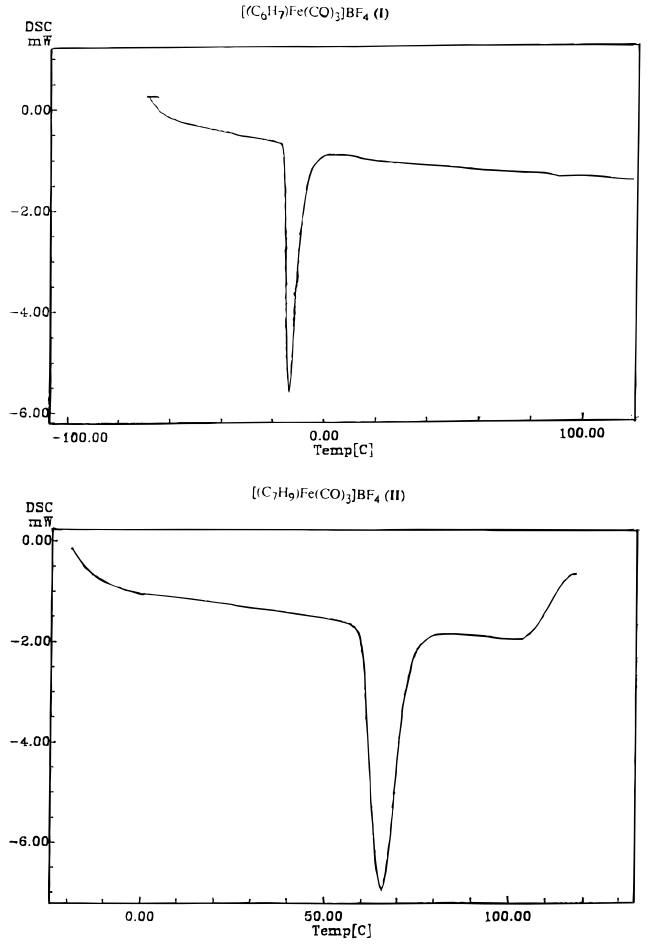

Figure 7. Differential scanning calorimetry traces for **I** and **II**. The heating rate was 10 K/min in both cases.

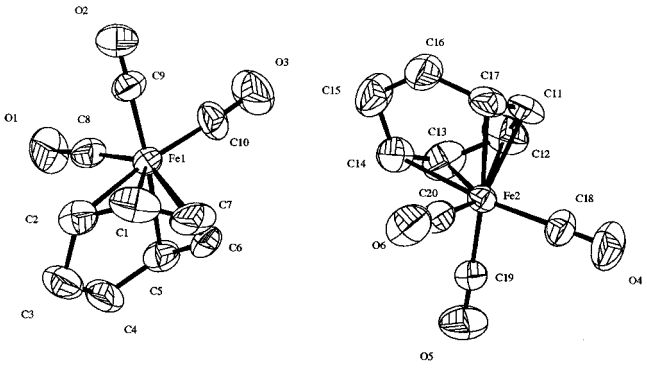

Figure 8. Structure of **II** showing thermal ellipsoids (50% probability). BF_4^- ions and hydrogen atoms are omitted for clarity.

any changes that might be responsible for the irreproducibility of ^1H T_1 measurements discussed above. In addition to the main phase transitions shown in Figure 7, extra weak endotherms and exotherms were observed. These were neither reversible nor completely reproducible, suggesting some small degree of irreversible structural change at 423 K.

X-ray Crystallography. The structure of **II** at 295 K is shown in Figure 8, and numerical details are given in Tables 4 and 5. The unit cell is tetragonal with two cycloheptadienyliron tricarbonyl cations in the asymmetric unit and electroneutrality maintained by two tetrafluroborate anions. The bond lengths are all within the expected ranges, and the structure is similar to the published structure of $(C_6H_7)Mn(CO)_3$.[42] The $[(C_7H_9)Fe(CO)_3]^+$ cations pack along the tetragonal *c* axis such that carbonyls face carbonyls and cyclodienylium rings face cyclodienylium rings, separated by the BF_4^- anions (see Figure 9, though the BF_4^- anions are omitted here for clarity). The $[(C_7H_9)Fe(CO)_3]^+$ cations show intermolecular bonding to the fluorines of the BF_4^- anions. One BF_4^- anion centered at B(1) shows intermolecular contacts through fluorine atoms to six $[(C_7H_9)Fe(CO)_3]^+$ cations with similar contact distances to both carbon and oxygen atoms in the respective carbonyls, F−C 2.98−3.46 Å and F−O 2.90−3.34 Å. There are also slightly longer contacts to ring carbon atoms F−C 3.31−3.48 Å. This counterion is more closely associated with two molecular cations with center to center contacts B(1)−Fe(1) 4.63 and B(1)−Fe(2)

(42) Churchill, M. R.; Scholer, F. R. *Inorg. Chem.* **1969**, *8*, 1950.

Table 4. Final Refined Non-Hydrogen Atomic Parameters ($\times 10^4$) and Equivalent Isotropic Thermal Parameters ($Å^2 \times 10^3$) for $[(C_7H_9)Fe(CO)_3]BF_4$ (**II**)

	x	y	z	*U*(eq)[a]
Fe(1)	7278(1)	2634(1)	285(1)	37(1)
Fe(2)	2370(1)	7720(1)	1030(1)	36(1)
F(1)	7826(19)	1668(9)	−1466(7)	175(8)
F(2)	6744(20)	2756(22)	−2175(11)	266(15)
F(3)	7507(35)	3442(16)	−1429(8)	339(23)
F(4)	8561(12)	2996(34)	−2032(15)	363(24)
F(5)	2488(26)	1463(29)	1207(9)	251(13)
F(6)	3303(20)	3075(10)	919(10)	188(9)
F(7)	3918(10)	1169(12)	591(12)	189(8)
F(8)	1957(16)	1762(24)	388(9)	218(12)
B(1)	7654(12)	2655(12)	−1831(9)	45(2)
B(2)	3057(20)	2037(18)	658(13)	94(6)
O(1)	9689(8)	2628(11)	−374(5)	86(3)
O(2)	6020(9)	664(9)	−441(5)	77(3)
O(3)	5966(11)	4530(9)	−465(6)	88(3)
O(4)	466(9)	9069(10)	1768(6)	89(3)
O(5)	4292(10)	8985(10)	1760(5)	89(3)
O(6)	2364(12)	5337(9)	1701(4)	88(3)
C(1)	6865(13)	1548(14)	1036(7)	71(4)
C(2)	8142(12)	1318(10)	929(6)	58(3)
C(3)	9263(13)	1948(11)	1288(6)	68(3)
C(4)	9330(12)	3257(12)	1216(7)	69(3)
C(5)	8310(10)	3924(10)	901(6)	53(3)
C(6)	7052(11)	3786(15)	1055(7)	70(4)
C(7)	6377(13)	2645(17)	1132(6)	77(4)
C(8)	8724(12)	2644(11)	−132(5)	55(3)
C(9)	6483(11)	1409(9)	−162(5)	52(2)
C(10)	6484(9)	3831(11)	−168(6)	55(3)
C(11)	1164(13)	7971(13)	275(7)	66(3)
C(12)	2328(15)	8671(12)	176(7)	73(4)
C(13)	3516(12)	8142(13)	280(7)	67(3)
C(14)	3684(10)	6869(13)	377(6)	62(3)
C(15)	3105(12)	5764(15)	30(7)	76(4)
C(16)	1714(11)	5662(15)	109(8)	80(5)
C(17)	1069(9)	6701(12)	416(6)	57(3)
C(18)	1177(10)	8537(9)	1492(6)	54(3)
C(19)	3581(10)	8544(11)	1472(6)	54(3)
C(20)	2361(11)	6269(9)	1460(5)	50(2)

[a] *U*(eq) is defined as one-third of the trace of the orthogonalized U_{ij} tensor.

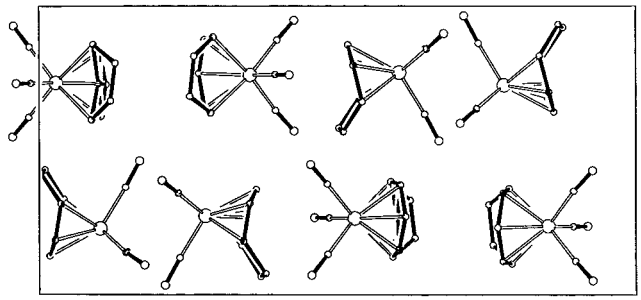

Figure 9. View along the *a* axis of the (tetragonal) unit cell of **II**. BF_4^- anions are omitted for clarity; the *c* axis is the horizontal axis.

Table 5. Selected Bond Lengths (Å) and Angles (deg) for $[(C_7H_9)Fe(CO)_3]BF_4$ (**II**)

Fe(1)−C(8)	1.782(12)	Fe(1)−C(10)	1.815(11)
Fe(1)−C(9)	1.829(11)	Fe(1)−C(1)	2.047(13)
Fe(1)−C(7)	2.076(13)	Fe(1)−C(6)	2.087(12)
Fe(1)−C(2)	2.180(13)	Fe(1)−C(5)	2.206(11)
Fe(2)−C(20)	1.802(10)	Fe(2)−C(19)	1.828(11)
Fe(2)−C(18)	1.834(11)	Fe(2)−C(13)	2.085(13)
Fe(2)−C(11)	2.100(12)	Fe(2)−C(12)	2.115(14)
Fe(2)−C(14)	2.187(11)	Fe(2)−C(17)	2.204(11)
C(8)−Fe(1)−C(10)	96.8(5)	C(8)−Fe(1)−C(9)	97.5(5)
C(10)−Fe(1)−C(9)	89.7(5)	C(8)−Fe(1)−C(1)	126.5(6)
C(10)−Fe(1)−C(1)	136.7(5)	C(9)−Fe(1)−C(1)	85.8(6)
C(8)−Fe(1)−C(7)	148.0(6)	C(10)−Fe(1)−C(7)	105.3(6)
C(9)−Fe(1)−C(7)	105.3(6)	C(1)−Fe(1)−C(7)	36.5(6)
C(8)−Fe(1)−C(6)	120.3(5)	C(10)−Fe(1)−C(6)	88.4(6)
C(9)−Fe(1)−C(6)	142.1(5)	C(1)−Fe(1)−C(6)	70.4(7)
C(7)−Fe(1)−C(6)	39.8(6)	C(8)−Fe(1)−C(2)	88.2(5)
C(10)−Fe(1)−C(2)	172.9(5)	C(9)−Fe(1)−C(2)	94.6(4)
C(1)−Fe(1)−C(2)	38.5(5)	C(7)−Fe(1)−C(2)	68.1(6)
C(6)−Fe(1)−C(2)	84.7(6)	C(8)−Fe(1)−C(5)	83.0(5)
C(10)−Fe(1)−C(5)	97.2(5)	C(9)−Fe(1)−C(5)	173.0(5)
C(1)−Fe(1)−C(5)	88.3(5)	C(7)−Fe(1)−C(5)	71.7(5)
C(6)−Fe(1)−C(5)	37.5(5)	C(2)−Fe(1)−C(5)	78.4(4)
C(20)−Fe(2)−C(19)	98.0(5)	C(20)−Fe(2)−C(18)	96.7(5)
C(19)−Fe(2)−C(18)	88.4(5)	C(20)−Fe(2)−C(13)	126.4(5)
C(19)−Fe(2)−C(13)	84.2(6)	C(18)−Fe(2)−C(13)	136.9(5)
C(20)−Fe(2)−C(11)	120.8(6)	C(19)−Fe(2)−C(11)	141.2(6)
C(18)−Fe(2)−C(11)	87.0(6)	C(13)−Fe(2)−C(11)	73.4(6)
C(20)−Fe(2)−C(12)	149.7(6)	C(19)−Fe(2)−C(12)	104.4(6)
C(18)−Fe(2)−C(12)	104.0(6)	C(13)−Fe(2)−C(12)	38.9(6)
C(11)−Fe(2)−C(12)	40.4(6)	C(20)−Fe(2)−C(14)	89.3(5)
C(19)−Fe(2)−C(14)	95.3(5)	C(18)−Fe(2)−C(14)	172.5(5)
C(13)−Fe(2)−C(14)	37.6(5)	C(11)−Fe(2)−C(14)	86.1(6)
C(12)−Fe(2)−C(14)	68.8(6)	C(20)−Fe(2)−C(17)	83.8(5)
C(19)−Fe(2)−C(17)	173.6(5)	C(18)−Fe(2)−C(17)	97.5(5)
C(13)−Fe(2)−C(17)	89.7(5)	C(11)−Fe(2)−C(17)	37.5(5)
C(12)−Fe(2)−C(17)	71.8(5)	C(14)−Fe(2)−C(17)	78.6(4)

4.66 Å; further contacts to another four cations complete a pseudooctahedral geometry, B(1)−Fe 5.33−5.39 Å. The second BF_4^- anion centered around B(2) also shows intermolecular contacts to six cations. The orientation with respect to the $[(C_7H_9)Fe(CO)_3]^+$ cations is different in this counterion with several short contacts to ring carbons, F−C 3.26−3.48 Å. This BF_4^- anion also shows contacts to several carbonyl oxygens, two of which are purely associated with the oxygens, F−O 3.07−309 Å, and two of which also show contacts to the respective carbonyl carbons, F−O 3.24, 3.47 and F−C 3.34, 3.35 Å. This counterion is again more closely associated with two cations with B(2)−Fe(1) 4.59 and B(1)−Fe(2) 4.71 Å; a further four cations complete a pseudooctahedral geometry with center to center contacts, B(2)−Fe 6.13−6.32 Å. The relatively high thermal parameters on the fluorine atoms reflect positional/motional disorder on these atoms; see Table 4. There are no significant structural differences between the molecules in the asymmetric unit; the molecular geometry is summarized in Table 5.

The X-ray powder patterns of **I** and **II**, at room temperature, are noticeably similar with several coincident lines, Figure 10. The powder pattern for **II** can be indexed successfully on the tetragonal cell found in the single-crystal determination, confirming the phase purity of the powder. The pattern for **I** contains fewer lines, indicating a higher symmetry, but all the lines present in this pattern are observed also in the pattern of **II**, indicating a structural relationship between the two solids. The pattern for **I** was successfully indexed on a face-centered cubic cell with $a = 10.59(1)$ Å. This corresponds to approximately half the volume of the tetragonal unit cell found for **II**, suggesting that the structure of **I** is related to a disordered form of the structure of **II**. Measurement of the powder

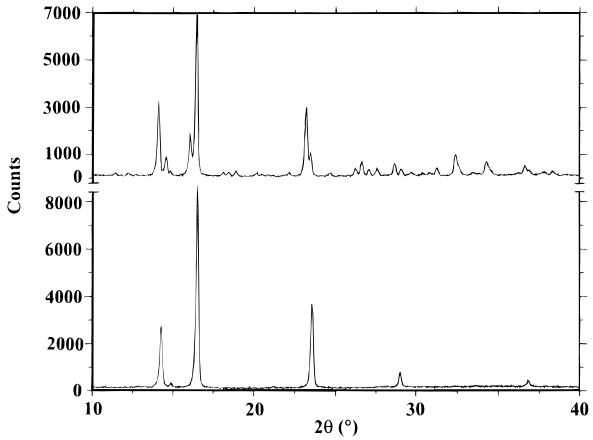

Figure 10. Powder X-ray diffraction patterns of **I** (lower) and **II** (upper) at 295 K.

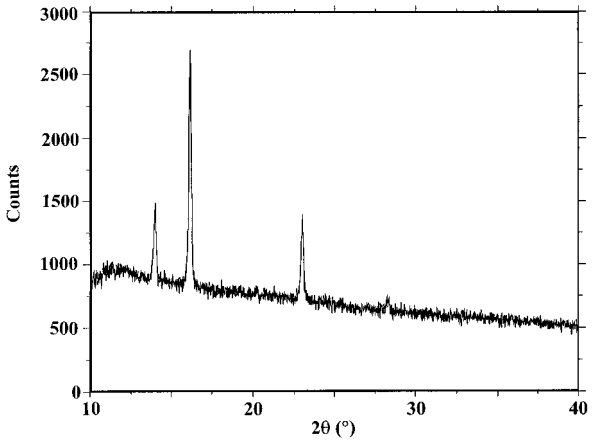

Figure 11. Powder X-ray diffraction pattern of **II** at 353 K.

diffraction pattern of **II** at elevated temperature, Figure 11, appears to confirm this close structural relationship, with a cubic cell ($a = 11.03(6)$ Å) found above 353 K. Attempts to measure single-crystal diffraction data for **II** at this temperature were unsuccessful, with a loss of crystallinity observed.

Discussion

The variable-temperature NMR spectra clearly show that both complexes undergo motion in the solid state. This, in conjunction with the fact that the complexes are isomorphous in their dynamic regimes and are also likely to be so in their static regimes, indicates that the motions involved are similar in both cases. The barrier to motion is clearly greater in complex **II**, as the onset of the motion, specifically the narrowing of the ^1H and ^{13}C resonances, occurs at higher temperatures.

One could envisage several ways in which such molecules could undergo dynamic behavior, without ligand exchange or other highly energetic process such as cation exchange: (a) a static $Fe(CO)_3$ moiety with dynamic ring rotation about the pseudo-3-fold axis; (b) a static Fe and ring moiety with dynamic interchange of CO groups about the pseudo-3-fold axis; (c) a combination of (a) and (b) about the pseudo-3-fold axis; (d) a general rotation, or molecular tumbling, of the entire molecule about any axis centered on Fe. The observation, in the section on the ^{13}C NMR spectra, that the carbonyl and ring resonances narrow (become motional) over the same temperature range excludes mechanisms a and b.

A close examination of the unit cell of **II** (from the single-crystal determination at room temperature) is quite informative. Figure 9 is a view along the *a* axis of the tetragonal unit cell,

with the BF_4^- counterions omitted for clarity. The long *c* axis is halved in length above the phase transition. In order to accomplish this, there must be a reorientation of the molecules in the unit cell and thus the motion is not simply about the $Fe(CO)_3$ pseudo-3-fold axis, excluding mechanism c. The fact that a crystalline powder diffraction pattern is observed for both complexes in the dynamic regime, with no evidence in the background of significant diffuse scattering, indicates that, despite the dynamic reorientational behavior of these systems, the atoms are on average located in defined crystallographic sites. The motion is therefore likely to involve an intersite hopping mechanism. This fact, in conjunction with the low activation energy estimated from the T_1 study and the surprisingly low ^{13}C chemical shift anisotropies observed in the static ^{13}C spectra of **I** and **II** (dynamic regimes), strongly suggests that the molecules are undergoing rapid molecular tumbling in their dynamic regimes, mechanism d. This is somewhat surprising considering that none of the (arene)$M(CO)_3$ complexes studied so far behave in this way[10] and that the unit cell is quite compact, Figure 9. Whole-molecule tumbling is consistent with the barrier to motion being greater in complex **II**, as it has the bulkier ring.

The ^1H and ^{13}C NMR studies on **I** and **II** in their dynamic regimes show that, on reduction of the temperature below the phase transition, the complexes become static again; it is reasonable to assume that the crystallographic change associated with the onset of motion is reversible also. Thus it is likely that the packing arrangements in the two regimes are closely related and easily interconverted. Knowing that **II** is tetragonal at room temperature, the X-ray diffraction patterns of **I** and **II** in their motional regimes were successfully fitted to face-centered cubic unit cells. Thus, when compound **II** is heated above the phase transition, the tetragonal unit cells become cubic; the unit cell now contains four molecules and the asymmetric unit contains a single molecule of **II** and a BF_4^- counterion. We anticipate that at low temperatures the structure of **I** also reverts to a low-symmetry tetragonal cell.

Some degree of irreversible structural change after heating to high temperatures was indicated by both the ^1H relaxation time and the DSC experiments. Some loss in crystallinity in X-ray measurements performed on heated samples was also observed. It is difficult to account for such changes occurring well below the bulk decomposition temperature. However, one could speculate that a cause might be partial trapping of some molecules in the unit cell in the wrong conformation.

Conclusions. The complexes $[(C_6H_7)Fe(CO)_3]BF_4$ and $[(C_7H_9)Fe(CO)_3]BF_4$ both undergo a phase transition to become dynamic in the solid state at high temperature. The temperature of the phase transition is higher for the cycloheptadienyl complex, suggesting that the barrier to the motion is greater for the more sterically hindered cation. The motion is shown to involve rapid reorientation of the whole molecule.

Acknowledgment. We are grateful to the EU, which provided a postdoctoral fellowship for D.F.B. under the Human Capital and Mobility Programme and general support for G.E.H. We thank the University of London Intercollegiate Research Service for providing NMR spectrometer time and Ms. M. Odlyha of the ULIRS for providing DSC facilities. Finally, we thank Dr. Tracey Kelly (University College Dublin) for her synthetic work on our behalf.

Supporting Information Available: Tables giving full structural refinement information, complete bond lengths and angles, atomic coordinates for all atoms, and anisotropic displacement parameters for all non-hydrogen atoms (10 pages). Ordering information is given on any current masthead page.

IC951573T